Macromolecules

Article

pubs.acs.org/Macromolecules

Light-Driven Living/Controlled Radical Polymerization of Hydrophobic Monomers Catalyzed by Ruthenium(II) Metalacycles

Nelson Vargas Alfredo,[†] Noel Espinosa Jalapa,[‡] Salvador Lopez Morales,[†] Alexander D. Ryabov,[§] Ronan Le Lagadec,*[,‡] and Larissa Alexandrova*[,†]

[†]Instituto de Investigaciones en Materiales, Universidad Nacional Autónoma de México, Circuito Exterior s/n, Ciudad Universitaria, 04510, México D.F., Mexico

[‡]Instituto de Química, Universidad Nacional Autónoma de México, Circuito Exterior s/n, Ciudad Universitaria, 04510, México D.F., Mexico

[§]Department of Chemistry, Carnegie Mellon University, 4400 Fifth Avenue, Pittsburgh, Pennsylvania 15213, United States

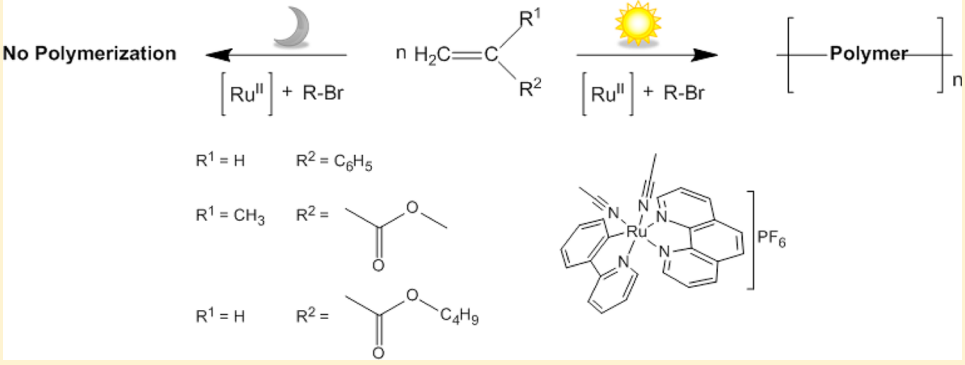

ABSTRACT: A versatile photoactivated catalytic system based on a cyclometalated ruthenium(II) complex, composed of strongly coordinating bidentate and relatively labile ligands, in conjunction with a traditional alkyl bromide initiator, has been developed for living/controlled radical polymerization. Polymerizations of three typical hydrophobic monomers—methyl methacrylate (MMA), styrene (St), and *n*-butyl acrylate (BA)—proceeded to high conversions under visible light irradiation. The polymerization process was photoresponsive, i.e., took place only under irradiation and immediately stopped when the light was turned off. Block copolymers of MMA with St and BA with St, as well as statistical copolymer of BA and St, could also be conveniently prepared. ^{1}H NMR and electrochemical studies suggest a mechanism of the catalytic activation, which involves a photoinduced formation of the solvento 18-electron species *cis*-[Ru(*o*-C_6H_4-2-py)(phen)(MeCN)(acetone)]$^+$ through the intermediacy of the 16-electron five-coordinated complex *cis*-[Ru(*o*-C_6H_4-2-py)(phen)(MeCN)]$^+$ which is believed to be a crucial intermediate of the overall ATRP process.

INTRODUCTION

Remarkable progress in the development of catalytic systems for metal-catalyzed or atom transfer radical polymerization (ATRP) has been achieved since its discovery in 1995.[1,2] The existing methodologies allow the synthesis of well-defined polymer structures of predictable molecular weights and narrow polydispersities using extremely low (ppm) concentrations of transition metal catalysts.[3−7] Furthermore, newly developed catalysts permit living/controlled polymerizations of numerous functional and hydrophilic monomers,[6−11] many of which were considered as problematic for this technique and whose controlled polymerization was hardly possible using initial version of the Ru^{II}- or Cu^{I}-based catalytic systems. A large variety of complexes of different transition metals as effective ATRP catalysts have been reported;[6−11] however, development of new active and versatile catalysts is still a vigorous subject of study. Recently, photocatalysis has been attracting a great deal of attention because of environmental and energy resource problems. Ruthenium compounds, particularly the Ru^{II} complexes, have been known for decades because of their extremely interesting light sensitivity. They still play a key role in the development of different aspects of photophysics and photochemistry.[12] On the other hand, Ru^{II} complexes are very extensively applied as catalysts in polymerization reactions such as metathesis[13−15] and ATRP.[6−11,16] Similarly, photoactivated metathesis polymerizations have been reported by various authors,[15,17−20] with Ru^{II}-based complexes being used as precatalysts in most of the cases, but the polymerizations have also been observed with tungsten,[21] molybdenum,[22] and rhenium[23] complexes. The application of light-driven catalytic systems in ATRP has been very limited. Many of the reported highly effective ATRP catalysts were formed *in situ* using

Received: July 11, 2012
Revised: September 21, 2012
Published: October 8, 2012

   dx.doi.org/10.1021/ma3014383 | *Macromolecules* 2012, 45, 8135−8146

thermally triggered precursors.[3,24−30] An attempt of photoactivation of the dimeric $[RuCl_2(1,3,5\text{-}C_6H_3iPr_3)]_2$ in atom transfer radical addition (ATRA), a reaction mechanistically very similar to ATRP, was made, but the procedure was not successful.[26] Although several papers on photo-ATRPs have been published, UV irradiation was used for cleavage of a special photosensitive initiator or photoiniferter (dithiocarbamate) but not for activation of the metal catalysts.[31,32] We have found only one successful example of a light-driven catalytic system in ATRP with alkyl halide (iodide) initiator,[33,34] where the dinuclear manganese carbonyl complex, $[Mn_2(CO)_{10}]$, underwent photochemical homolysis to generate highly reactive catalytic species, which was able to mediate polymerizations of various vinyl monomers under very mild conditions with good control. Although the authors proposed that the manganese complex served as a simple radical generator and the polymerization was controlled by a degenerative iodine transfer, the possibility of operation by the ATRP mechanism cannot be discarded. During the preparation of this article a paper was published which reported the photoinduced ATRP of MMA based on the photogeneration of a Cu^I active catalyst from a much more stable Cu^{II} complex[35] using an alkyl halide as the initiator. It was reported that the polymerization proceeded with good control and did not require the use of any reducing additives.

Recently, ATRP of different vinyl monomers catalyzed by cyclometalated Ru^{II} complexes has been reported by our group.[36−38] In contrast to the majority of the ruthenium catalysts applied,[11,16,39] these complexes are cationic 18-electron, octahedral, chloride- and phosphine-free compounds. They demonstrated surprisingly high activity in the polymerizations though they were coordinatively saturated structures with relatively strongly bound ligands. Application of such coordinatively saturated complexes in ATRP can be both advantageous and disadvantageous in comparison with coordinatively unsaturated or easily labile compounds. The activity of the catalyst is directly related to the ability to incorporate halogen atom from the initiator (normally an alkyl halide). A vacant site within the coordination sphere makes unsaturated complexes catalytically more active because no ligand elimination is needed.[40−44] However, unsaturated complexes are often less stable and therefore more difficult to handle. A successful strategy may be a certain combination of strongly coordinating and labile ligands that facilitates the formation of the appropriate highly active catalyst *in situ* from a stable precursor.[26,27,45,46] The use of UV−vis light for activating precatalyst is in many ways better than a thermal activation. Usually, photochemical reactions occur at low temperatures; they are energetically efficient and more selective than thermally initiated processes.

Within the series of cyclometalated Ru^{II} compounds synthesized by our group, photosensitive complexes have also been described.[47] These are ruthenacycles of 2-phenylpyridine, bearing one chelate, 1,10-phenanthroline (phen) or 2,2′-bipyridine (bpy), and two cis-coordinated MeCN ligands of general formula *cis*-$[Ru(o\text{-}C_6H_4\text{-}2\text{-}py)(LL)(MeCN)_2]PF_6$, where LL = phen (I) or bpy (II) (see Scheme 1 for the structures). The complexes are thermally very stable in the solid state and in solution, but irradiation with visible light in methanol led to substitution of MeCN ligands by MeOH within a few minutes and generation of species with a much lower reduction potential. Thus, these photosensitive complexes readily produce novel compounds of higher reduction power which may be very active catalysts in ATRP. In this paper, we focus on one of such complexes, *cis*-$[Ru(o\text{-}C_6H_4\text{-}2\text{-}py)(phen)(MeCN)_2]PF_6$ (**I**), as a phototriggered precatalyst for controlled/living radical polymerization of various hydrophobic monomers.

Scheme 1. Structures of the Cyclometalated Ruthenium(II) Complexes I and II

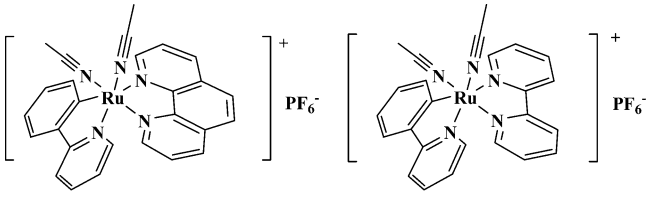

I II

EXPERIMENTAL SECTION

Materials. All reagents were purchased from Aldrich Chemical Co. The monomers MMA, St, and BA were washed with NaOH solution 10% (w/v), passed through a column filled with neutral alumina, and distilled under reduced pressure. Acetone (99.9+%), methyl ethyl ketone (MEK) (99.9+%), and dichloromethane (99.9%) were distilled prior use; *N*,*N*-dimethylformamide (DMF) (HPLC grade), toluene (99.9%), THF (HPLC grade), and ethyl 2-bromoisobutyrate (EB*i*B) (98%) were used as received.

Synthesis of Ru Complexes. The complexes *cis*-$[Ru(o\text{-}C_6H_4\text{-}2\text{-}py)(phen)(MeCN)_2]PF_6$ (**I**) and *cis*-$[Ru(o\text{-}C_6H_4\text{-}2\text{-}py)(bpy)(MeCN)_2]PF_6$ (**II**) were prepared according to the literature.[47]

Polymerization Procedure under Visible Light Irradiation. The polymerizations were carried out in an argon atmosphere in 15 mL Schlenk glass tubes provided with stir bars, under irradiation from Cole-Parmer DC-Regulated Fiber Optic Illuminator System with a high-intensity bulb of 150 W (λ from 400 to 900 nm) and self-supporting flexible gooseneck light pipes with lens to provide a well-defined illumination. The distance between the reaction tube and the light source was kept at 2.5 cm. All polymerizations were performed in solution (monomer/solvent 50% v/v) with EB*i*B as an initiator. The initial molar ratio of $[monomer]_0/[EBiB]_0/[Ru^{II}]_0$ = 200/1/1 was used in the majority of the procedures. A typical example for MMA polymerization with precatalyst **I** is given below. **I** (31.7 mg, 0.048 mmol) was added to a Schlenk tube under constant flow of argon, and then MMA (1.0 mL, 9.578 mmol), acetone (1.0 mL, 13.619 mmol), and *n*-decane (0.10 mL) were introduced using a syringe; the mixture was degassed by three freeze−pump−thaw cycles. At the end EB*i*B (0.007 mL, 0.048 mmol) was added, and the tube was exposed to irradiation from the lamp. Samples were taken periodically using a N_2-purged syringe, then mixed with THF, passed through a column filled with Florisil (diameter = 13 mm, *h* = 25 mm) to remove the catalyst, and analyzed by GPC.

The polymerization of St was carried out in a similar way, but MEK was used instead of acetone, and the reaction tube was placed in a thermostatic quartz water bath at 60 °C.

Synthesis of Copolymers. *Block Copolymer of PMMA with PSt.* MMA was first photopolymerized with **I** and EB*i*B in acetone under conditions described above for the homopolymerization. The irradiation was turned off after 0.5 h (7% conversion), and the polymer was purified and characterized by GPC (M_n = 3300 and PDI = 1.50). Then, thus-obtained PMMA (94 mg, 0.028 mmol) was employed as macroinitiator in the polymerization of St (0.6 mL, 5.70 mmol) with **I** (18.90 mg, 0.028 mmol) in MEK (0.6 mL, 6.70 mmol) under irradiation using the following conditions: $[St]_0/[PMMA]_0/[I]_0$ = 200/1/1; St/MEK 50% v/v; 60 °C, Ar, *n*-decane (0.06 mL). The irradiation was turned off after 8 h. Conversion was determined by the GC method. The polymer was purified from the catalyst as above and analyzed by GPC and ^1H NMR.

dx.doi.org/10.1021/ma3014383 | *Macromolecules* 2012, 45, 8135−8146

Table 1. Thermopolymerizations Mediated by I and II in Toluene[a]

monomer	Cat.	T (°C)	time (h)	conv (%)	$M_{n,GPC} \times 10^{-3}$	$M_{n,th} \times 10^{-3}$	PDI
St	**I**	100	6	72	15.9	14.4	1.22
MMA	**I**	80	6	68	11.4	13.8	1.24
	II	80	6	55	8.9	11.2	1.33

[a]Conditions: $[\text{monomer}]_0/[\text{Ru}^{II}]_0/[\text{EB}i\text{B}]_0$ = 200/1/1; monomer/toluene = 50% v/v.

Block Copolymer of PBA with PSt. BA (0.8 mL, 5.461 mmol) was photopolymerized at room temperature with **I** (18.8 mg, 0.027 mmol) and EB*i*B (0.004 mL, 0.027 mmol), under conditions analogous to those described for the homopolymerization of MMA, but in MEK (0.8 mL, 8.93 mmol) instead of acetone. The light was turned off after 8 h, and samples for GC and GPC analysis were taken using a N_2-purged syringe. According to GC analysis, conversion of 90% was achieved, and no traces of EB*i*B were detected. GPC showed bimodal MWD for the synthesized PBA with the principal peak from lower molecular fraction (M_n = 32 300 and PDI = 1.60) and the secondary one of very high molecular weight ($M_n \approx 3 \times 10^6$). Then, the previously degassed St (0.6 mL, 5.461 mmol) and solution of **I** (8.0 mg, 0.012 mmol) in MEK (0.6 mL, 6.697 mmol) were added to the polymerized BA solution. The reaction mixture was placed in a water quartz bath at 60 °C and exposed to the irradiation for another 14 h. The polymer was purified and analyzed by GPC and ^{1}H NMR techniques. Conversion of ∼45% was achieved during the second polymerization of St. Composition of St−BA copolymer was obtained from GC data and compared with composition measured directly by ^{1}H NMR according to the relationship

$$F_{St} = \frac{2I(-C_6H_5)}{2I(-C_6H_5) + 5I(-CO_2CH_2\text{-})}$$

Simultaneous Copolymerization of BA and St. The procedure was very similar to that for the homopolymerization with precatalyst **I** (24.1 mg, 0.036 mmol) and EB*i*B (0.005 mL, 0.036 mmol), the only difference being the mixture of two monomers, BA (0.8 mL, 5.46 mmol) and St (0.6 mL, 5.46 mM), was introduced into the Schlenk tube from the start. MEK (1.4 mL, 15.63 mmol) was used as a solvent (monomer feed/MEK = 50% v/v) and *n*-decane (0.14 mL) as an internal standard. Thus, the initial monomer feed composition was equimolar (f_{St} = 0.5; f_{BA} = 0.5) and the initial molar ratio of $[\text{monomer feed}]_0/[\mathbf{I}]_0$ was equal to 300/1 or $[BA]_0/[St]_0/[\text{EB}i\text{B}]_0/[\mathbf{I}]_0$ = 150/150/1/1. The polymerization mixture was irradiated for 10 h at room temperature. Total conversion determined on disappearance of both monomers was 24%. The obtained copolymer was purified the same way as described above and characterized by GPC and ^{1}H and ^{13}C NMR. The experiment was repeated using the same initial composition with irradiation performed at 60° using preheated water quartz bath.

Characterization. Monomer conversions were determined from the concentration of residual monomers by gas chromatography (GC), using a Shimadzu GC-2010 gas chromatograph equipped with one capillary column RESTEK stabilwax (30 m, 0.53 mm i.d., and 0.5 lmdf). *n*-Decane as an internal standard was added in every polymerization in a proportion of ∼10% to the monomer (v/v). Analysis conditions: injector temperature, 220 °C; temperature program, 4 min 40 °C, 15 °C/min until 220 °C, 2 min 220 °C.

The molecular weight and the molecular weight distributions of the polymers were determined by GPC chromatography on a Waters 2695 ALLIANCE separation module apparatus equipped with two HSP gel columns (HR MBL molecular weight range from 5×10^2 to 7×10^5 and MB-B from 10^3 to 4×10^6) in series and a RI Waters 2414 detector. THF was used as an eluent at 35 °C with a flow rate of 0.5 mL/min. Linear PMMA standards were utilized for the GPC calibrations.

Electrochemical measurements were performed on a PC-interfaced potentiostat−galvanostat AUTOLAB PGSTAT 12. A three-electrode setup was used with a BAS working glassy carbon electrode, Ag/AgCl reference electrode, and auxiliary Pt electrode. Before each measurement, the working electrode was polished with a diamond paste and rinsed with acetone and distilled water.

NMR spectra were obtained on a Bruker Avance 400 MHz spectrometer.

RESULTS AND DISCUSSION

General Observations. Both complexes, **I** and **II**, mediated radical polymerizations of St and MMA in toluene at 100 and 80 °C, respectively, with EB*i*B as an initiator. The main data of these polymerizations are given in Table 1.

Using the initial molar ratios of $[\text{monomer}]_0/[\text{Ru}^{II}]_0/[\text{EB}i\text{B}]_0$ = 200/1/1, the polymerizations were fast and reasonably controlled; i.e., the molecular weights grew proportionally to the conversion and were close to the calculated values assuming that one polymer chain was generated by one molecule of the initiator. The polydispersities (PDIs) were also quite narrow, particularly for PSt. The polymerizations catalyzed by **I** were faster, and the polymers of narrower PDIs were obtained.

The complexes are coordinatively saturated, and therefore, the dissociation of one of the ligands for their activation is required as it has been shown for other 18-electron ruthenium compounds.[26,27,45] Dissociation of one MeCN ligand is the most likely way of the activation. MeCN is more weakly bound than phen, and a signal from free MeCN was detected by ^{1}H NMR spectroscopy during polymerization.[38] The interval of 110−80 °C is a commonly employed temperature range for the saturated ruthenium complexes with relatively strongly bound ligands in ATRP of hydrophobic monomers.[27,28,36,37,40,45,46,48] The polymerizations catalyzed by coordinatively unsaturated complexes or complexes with extremely labile ligands occur at lower temperatures.[26,41,42]

Resistant to thermo-substitution, compounds **I** and **II** undergo readily photo-substitution under mild irradiation by visible light. The photosolvolysis of MeCN ligands occurs within several minutes in MeOH generating species of much lower reduction potential. Interestingly, the potential decreased by up to 800 mV (from 575 to −230 mV vs Ag/AgCl) for the complex **I** with the phen ligand because of the complete photosolvolysis of both MeCN ligands. The primary photoproduct of the bpy complex, **II**, was monosubstituted $[\text{Ru}^{II}(o\text{-}C_6H_4\text{-}2\text{-py})(\text{bpy})(\text{MeCN})(\text{MeOH})]^+$ species, and the drop in the reduction potential was less drastic: ca. 300 mV (from 578 to 270 mV vs Ag/AgCl). In contrast to Cu catalysts,[3,5,41] the activity of 18-electron ruthenium complexes in ATRP did not depend directly on their reducing power but was rather determined by the lability of ligands.[37,40,45,48−50] Remarkably, both the reducing power and lability of **I** and **II** can be simultaneously modified. A dramatic drop in the reduction potential was accompanied by the exchange of MeCN for much more labile MeOH ligand, and thus very active species were produced. The goal of the present study was to use the photolability of the MeCN ligands in order to form *in situ* active species which would be able to mediate living/controlled polymerization under mild conditions.

dx.doi.org/10.1021/ma3014383 | *Macromolecules* 2012, 45, 8135−8146

However, methanol cannot be used as solvent in the polymerization of hydrophobic monomers. Because of the low solubility at room temperature of the charged complexes in the majority of nonpolar organic solvents, polymerizations in toluene, anisole, or in the bulk were not good options either. At ambient temperature the complexes are well soluble in ketones, methylene chloride, and DMF which can be used as solvents in the polymerizations.

Thus, the polymerization of MMA with the initial molar ratio of $[MMA]_0/[Ru^{II}]_0/[EBiB]_0 = 200/1/1$ was attempted in these solvents (50% v/v) under visible light irradiation at room temperature. Careful measurements of the temperature in the reaction vessel showed that the reaction mixture was slightly heated to 33−35 °C upon irradiation. The data after 7 h of irradiation are presented in Table 2.

Table 2. Polymerization of MMA Mediated by I and II in Different Solvents under Visible Light Irradiation at Room Temperature[a]

solvent	Cat.	conv (%)	$M_{n,th} \times 10^{-3}$ (g/mol)	$M_{n,GPC} \times 10^{-3}$ (g/mol)	PDI
acetone	**I**	47	9.6	16.0	1.39
	II	26	5.4	9.2	1.46
dichloromethane	**I**	42	8.6	7.5	1.48
	II	30	6.2	5.1	1.46
DMF	**I**	24	4.9	5.4	1.68
	II	16	3.4	4.3	1.72

[a]Conditions: $[MMA]_0/[Ru^{II}]_0/[EBiB]_0 = 200/1/1$; MMA/solvent = 50% v/v; data taken after 7 h of irradiation.

The polymerization did proceed in all these solvents under homogeneous conditions and was faster in acetone and CH_2Cl_2 than in DMF, achieving conversion of more than 40% in 7 h. The polymer of higher molecular weight was obtained in acetone. Again, as in the thermopolymerization, complex **I** was more active and allowed a better control than **II**; all further experiments were conducted with precatalyst **I**.

The polymerization did not proceed without irradiation ("dark" conditions) even in refluxing acetone. Importantly, the polymerization did not occur under postirradiation conditions either, i.e., when the reaction was first irradiated for 0.5 h (7% conversion) and then kept at 40 °C for 8 h without irradiation; the polymerization stopped at 7% conversion and did not progress further. Thus, continuous irradiation is absolutely essential for the polymerization, and this makes the system mechanistically challenging because the light is needed not only for a single event formation of an active coordinatively unsaturated species but probably for its permanent generation.

The radical mechanism was verified by the radical scavenger methodology. In order to avoid strong absorption in the region where the complex absorbs, 1.1 equiv of 2,2-diphenyl-1-picrylhydrazyl (DPPH) was used instead of 2,2,6,6-tetramethyl-1-piperidinoxyl (TEMPO), which was used for this purpose in the thermo-polymerizations. The polymerization did not take place in the presence of the radical scavenger. Additionally, change of color from dark blue was noted, meaning free radical trapping by DPPH. It is worth noting that the polymerizations in acetone and DMF did not proceed in the presence of Ru complex and absence of EBiB and vice versa, but it was not the case in CH_2Cl_2. The polymerizations in this solvent proceeded at the same rate both in the presence and in the absence of EBiB. No photopolymerization occurred without precatalyst **I** in the reaction mixture. Chlorinated solvents are known to undergo decomposition upon UV irradiation generating chlorine atom and carbon-centered radicals,[51,52] but under irradiation by visible light the photolysis is very slow and, for example, CH_2Cl_2 may be used as a solvent in photopolymerizations under these conditions without causing noticeable side effects.[53] In our case ruthenium species generated by light may interact with CH_2Cl_2 in the same way as with an alkyl halide initiator, i.e., via an oxidative addition reaction producing initiating radicals. Since the polymerization in DMF was slow and afforded polymer of broad MWD in agreement with other ATRP reported in this solvent,[54] acetone was the solvent of choice.

Homopolymerizations of MMA, St, and BA. Semilogarithmic kinetic plots of the photopolymerization of MMA and evolution of the molecular weight characteristics with conversion together with the corresponding GPC traces are shown in Figures 1 and 2, respectively.

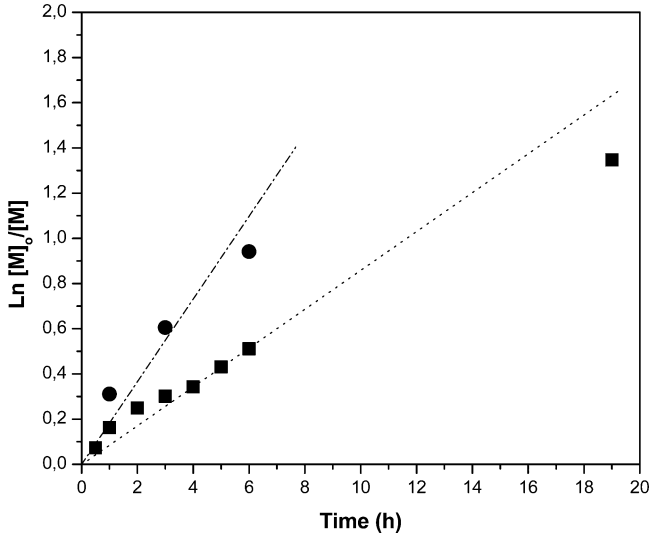

Figure 1. Kinetic plots for the EBiB initiated polymerization of MMA in acetone (MMA/acetone 50% v/v) with **I** under visible light irradiation at room temperature; $[MMA]_0/[I]_0/[EBiB]_0 = 200/1/1$ (■) and $MMA]_0/[I]_0/[EBiB]_0 = 200/1/2$ (●).

The kinetics may be approximated by a straight line passing through the origin, with a minor deviation from linearity at the beginning, which indicates a constant concentration of active species during the major time of the polymerization. The molecular weights increased linearly with the monomer conversion although remained higher than the values calculated based on 100% initiator efficiency (dashed line in Figure 2). Broad from the start, PDIs became narrower with conversion reaching values of 1.22. The total conversion of 74% was achieved after 19 h of irradiation. When the concentration of the initiator was increased 2-fold, the polymerization accelerated and PMMA of approximately twice lower molecular weight was obtained.

Two other typical monomers, BA and St, were also polymerized under the same conditions. The kinetic plots and evolution of the molecular weights for these polymerizations are presented in Figures 3 and 4, respectively.

In general, the photopolymerization of BA was much faster than that of MMA, achieving 91% conversion in 8 h, while St polymerized very slowly, resulting in only 6% conversion within

dx.doi.org/10.1021/ma3014383 | Macromolecules 2012, 45, 8135−8146

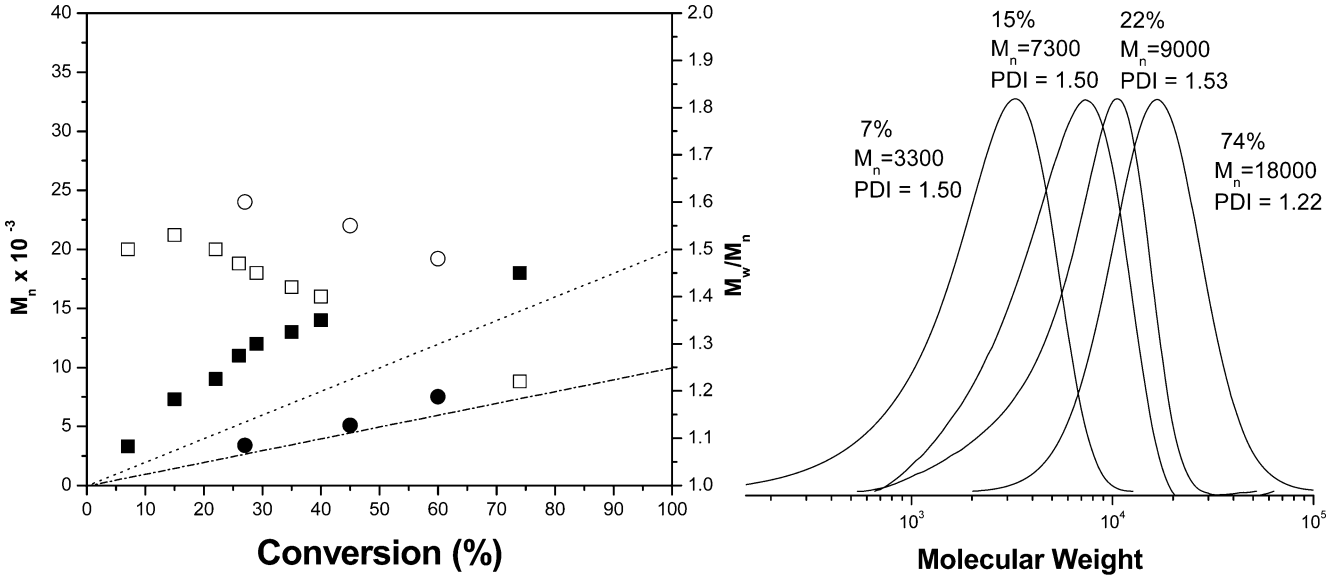

Figure 2. $M_{n,GPC}$, PDIs, and GPC traces of PMMA obtained with **I** and EB*i*B in acetone (MMA/acetone 50% v/v) under visible light irradiation at room temperature; $[MMA]_0/[\mathbf{I}]_0/[EBiB]_0 = 200/1/1$ (■, $M_{n,GPC}$; □, PDI) and $[MMA]_0/[\mathbf{I}]_0/[EBiB]_0 = 200/1/2$ (●, $M_{n,GPC}$; ○, PDI). Dashed and dot-dashed lines are shown for theoretical M_n calculated for $[MMA]_0/[EBiB]_0 = 200/1$ and 200/2, respectively.

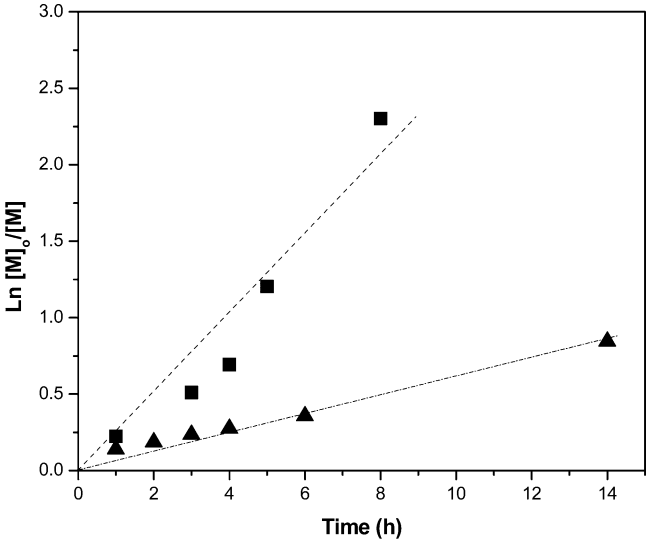

Figure 3. Kinetic plots of the EB*i*B initiated polymerizations of BA (■) in acetone at room temperature and St (▲) in MEK at 60 °C with **I** under visible light irradiation. Conditions: $[monomer]_0/[\mathbf{I}]_0/[EBiB]_0 = 200/1/1$; monomer/solvent 50% v/v.

the same period of time. In order to accelerate the St polymerization, the reaction mixture was heated to 60 °C and MEK was used instead of acetone. The conversions of 30% and 56% were obtained in 8 and 14 h, respectively, under continuous irradiation.

Again, no polymerization of St was observed under "dark" conditions, i.e., when the mixture was irradiated for 30 min and then immersed in a bath thermostatted at 70 °C for 12 h without irradiation. The GPC data showed that the molecular weights of both homopolymers, PSt and PBA, obtained in the photoprocesses were gradually shifted to higher values with conversion. PDIs also narrowed with conversion for PSt at least within 8 h of irradiation time. The polymerization of BA gave the polymer with the highest PDIs and besides revealed a bimodal distribution with a principal relatively narrow peak of lower molecular weight and a much broader secondary one of very high molecular weight ($M_n \approx 3 \times 10^6$). Relative intensity of the secondary peak developed progressively with conversion as seen from the GPC profiles obtained at different time of the polymerization (Figure 4). The distribution was practically monomodal after 1 h of irradiation, and then the higher molecular weight fraction appeared as a shoulder and finally as a secondary peak after 6 h of irradiation. Only $M_{n,GPC}$ of the low molecular weight fraction from GPC profiles of PBA were taken into account for plotting vs conversion in Figure 4. The increment in polydispersity index with conversion for PBA was rather due to the secondary peak. It is also possible that some acceleration observed in the polymerization of BA (Figure 3) is caused by development of this secondary polymerization. It is important to note that in contrast to the two other monomers, MMA and St, BA may be photopolymerized in the presence of the Ru complex without any initiator. Using the same catalyst concentration ratio as in other polymerizations, i.e., $[BA]_0/[\mathbf{I}]_0 = 200/1$, PBA of very high molecular weight with ~10% conversion was formed in 8 h. Its GPC curve corresponded well to the high molecular weight secondary peak presented in the GPC traces of PBA synthesized with EB*i*B (see Figure 4, dashed line in GPC traces of PBA). The ^{1}H NMR spectrum of this high molecular weight PBA did not reveal any difference in comparison with the spectrum of PBA obtained by free radical process.[55] The presence of 1 equiv of DPPH inhibited this polymerization as well. We did not investigate this process in detail, but this is a clear indication of two mechanisms operating in the polymerization. It is probable that both have a radical nature, but at this time we are unable to explain how the complex may generate a radical process in the absence of the alkyl halide. Bimodal GPC profiles in the radical polymerization of BA catalyzed by very active Ru^{II} half-sandwich complexes have previously been described in the literature, but no explanation of this fact was provided.[26,49] Thus, the observed behavior of BA is not only characteristic for our system; it may be general for the polymerizations catalyzed by certain Ru^{II} compounds, and its complete study is beyond the scope of this article. On the other hand, the secondary BA polymerization is

dx.doi.org/10.1021/ma3014383 | *Macromolecules* 2012, 45, 8135–8146

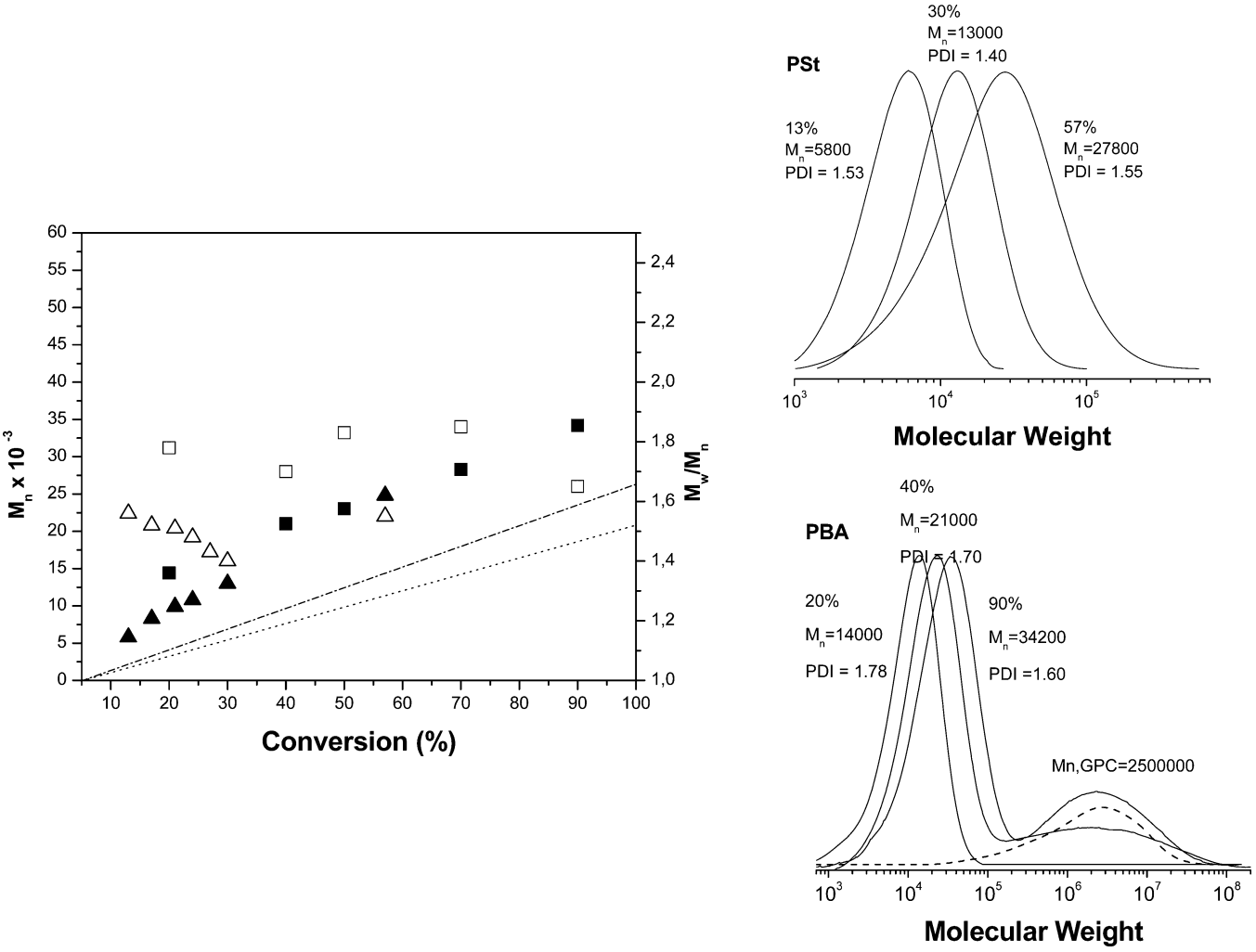

Figure 4. $M_{n,GPC}$, PDIs, and GPC traces of PBA (■, $M_{n,GPC}$; □, PDI) and PSt (▲, $M_{n,GPC}$; △, PDI) obtained with **I** and EB*i*B under visible light irradiation. Conditions: $[monomer]_0/[\mathbf{I}]_0/[EBiB]_0 = 200/1/1$; monomer/solvent 50% v/v; acetone, room temperature for PBA and MEK, 60 °C for PSt. Dashed and dot-dashed lines show theoretical M_n for PBA and PSt, respectively. GPC curve for PBA obtained in the absence of EB*i*B with pure **I** ($[BA]_0/[\mathbf{I}]_0 = 200/1$) in acetone (BA/acetone 50% v/v) at room temperature under visible light irradiation is given by dashed line within PBA GPC traces.

very slow when compared to the primary process under the investigated conditions used.

End-Group Analysis. The end-group analysis of the polymers was one of the principal methods for confirmation of the mechanism and evaluation of the degree of "livingness". The use of ^{1}H NMR to identify and quantify the end groups in PMMA obtained by ATRP is well-documented.[29,56] The ^{1}H NMR spectrum of PMMA ($M_{n,GPC}$ = 3800) obtained with **I** and EB*i*B after 35 min of visible light irradiation is shown in Figure 5. The spectrum is very similar to the previously reported data.[29,56] As well as the principal signals from the main-chain protons of PMMA (a, b, and c in Figure 5), we can also see small signals from the methylene protons of the ethyl ester group at the α-end at 4.10 ppm (e) and from the methoxy protons adjacent to the bromine atom at the ω-end at 3.75 ppm (d) on the shoulder of the peak of the main-chain methyl ester protons (c). The M_n calculated from the ratio of integral intensities of the main chain peak to the α-end signal (2c/3e) gave ~3600, which was in quite good agreement with that obtained from GPC. This result indicates that the polymerization proceeded through the activation of the EB*i*B C−Br bond to attach the ethyl ester at the α-end. However, the area

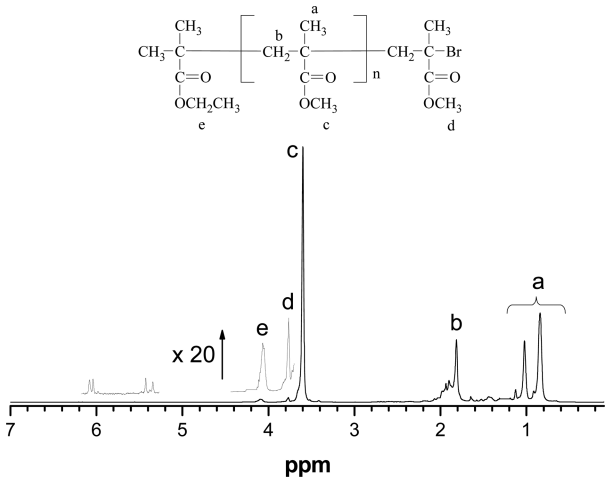

Figure 5. ^{1}H NMR spectrum in $CDCl_3$ of PMMA synthesized under visible light irradiation at room temperature with precatalyst **I** and EB*i*B.

dx.doi.org/10.1021/ma3014383 | *Macromolecules* 2012, 45, 8135−8146

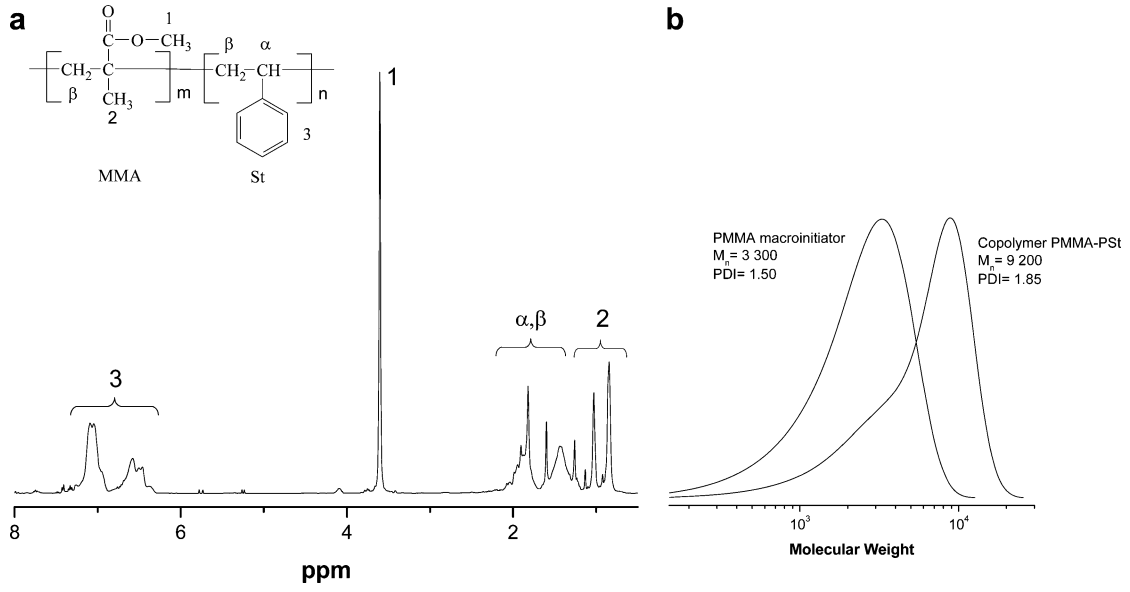

Figure 6. (a) ^{1}H NMR spectrum in CD_3Cl of PMMA-*b*-PSt obtained with **I** under visible light irradiation. (b) GPC traces of PMMA-macroinitiator and PMMA-*b*-PSt.

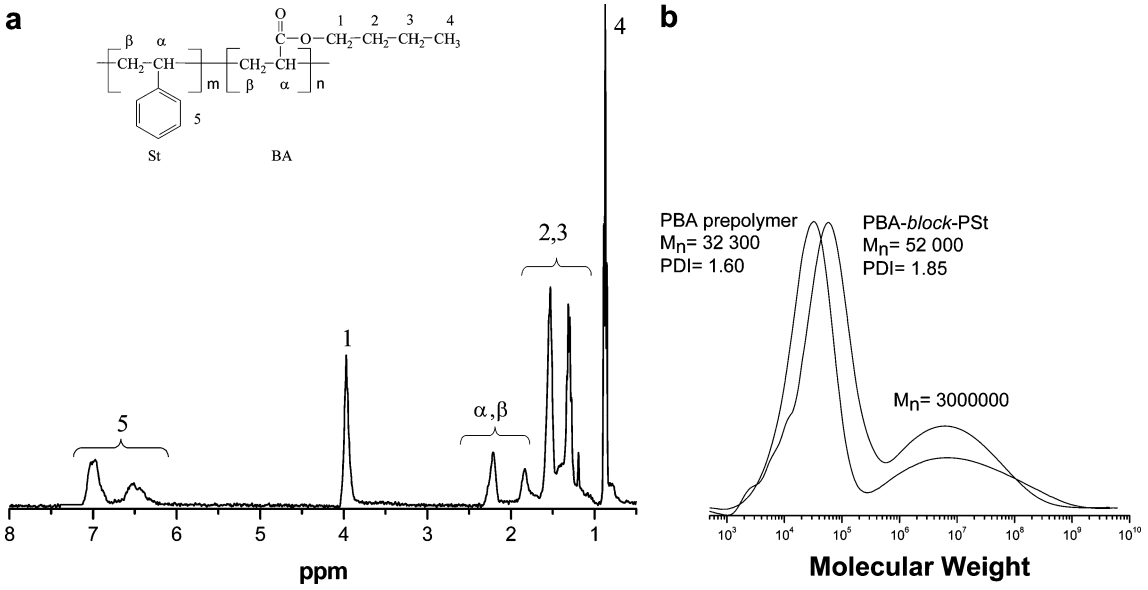

Figure 7. (a) ^{1}H NMR spectrum in $CDCl_3$ of PBA-*b*-PSt copolymer. (b) GPC traces of prepolymer of BA and PBA-*b*-PSt.

ratio between the α- and ω-end signals (e/d) was 2:2.5 instead of the expected values of 2:3. Additionally, very small signals at 5.44 and 6.11 ppm, assigned to the terminal olefinic methylene protons of unsaturated chain ends, are probably due to disproportionation. In conclusion, some irreversible termination reactions also occurred in the system under the investigated conditions.

Synthesis of Block Copolymers. The living nature of the photopolymerization was further verified by the synthesis of block copolymers, PMMA-*b*-PSt and PBA-*b*-PSt. Details of these syntheses are given in the Experimental Section. The copolymer of PMMA-*b*-PSt was synthesized under visible light irradiation using the PMMA-macroinitiator approach. First, PMMA of M_n = 3300 and PDI = 1.50 was synthesized under the conditions described for the homopolymerization of MMA. The reaction was stopped after 25 min of irradiation (7% conversion), and the polymer was purified from the catalyst and dried in vacuum. Then it was employed as an initiator instead of EB*i*B in the photopolymerization of St. The conditions of this second polymerization were very similar to those for the homopolymerization of St:MEK as a solvent (St/MEK = 50% v/v), 60 °C under visible light irradiation, $[St]_0/[I]_0/[PMMA]_0 \approx 200/1/1$. The reaction was stopped after 8 h (10% conversion); the polymer was purified from the catalyst, dried, and characterized by ^{1}H NMR and GPC. The results are depicted in Figure 6.

The characteristic signals from both PMMA and PSt are present in the NMR spectrum (Figure 5a). The molar fractions of F_{PSt} = 0.54 and F_{PMMA} = 0.46 were determined from the integration of the signals of PSt in the aromatic region ca. 6.4–7.1 ppm (5 protons) and the PMMA singlet at 3.6 ppm (3 protons from the methoxy group). An increase in the molecular weights from 3300 to 9100 after the second St polymerization was measured by GPC calibrated by PMMA standard, which

dx.doi.org/10.1021/ma3014383 | *Macromolecules* 2012, 45, 8135–8146

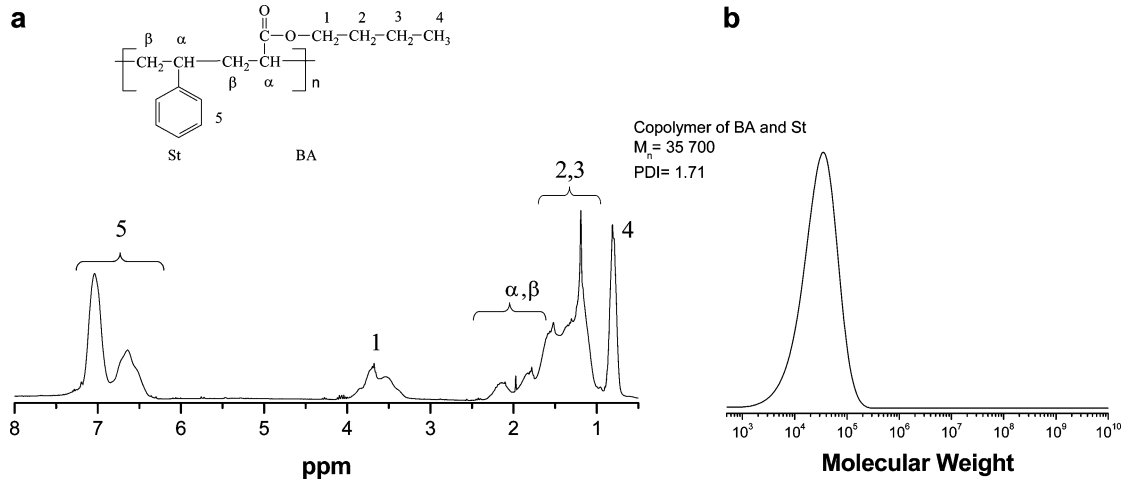

Figure 8. (a) ^{1}H NMR spectrum in $CDCl_3$ of copolymer of St and BA obtained by simultaneous polymerization under visible light irradiation at room temperature and (b) GPC traces of the copolymer.

generally gives about 30% higher molecular weight for PSt. Taking this into consideration, the GPC determined growth in the molecular weights agreed well with amount of St units in the copolymer obtained from the NMR data. The GPC curve of the copolymer revealed some asymmetry because of a tail from the PMMA dead chains, but the majority of the PMMA chains were successfully extended by St units. The occurrence of the irreversible terminal reactions during the photopolymerization of MMA was also deduced from the end-group analysis.

The sequential block copolymerization of BA and St was also examined. Since BA can be polymerized quantitatively within a short irradiation time, its copolymerization was performed without separation of the first PBA block. For this, BA was irradiated for 8 h in MEK at room temperature and after its nearly complete consumption (90% conversion, M_n = 32 300, and PDI = 1.60) a fresh feed of St, equimolar to BA, together with a new portion of **I** in MEK solution, were added by syringe into the system ($[St]_0/[I]_0$ = 500/1; St/MEK = 50% v/v), and the reaction mixture was irradiated again at 60 °C, i.e., under the conditions employed in the St homopolymerization. It is important to emphasize that prior to addition of St as a second monomer, we verified by GC that EB*i*B was absent in the polymerization system. The polymerization of St did proceed under these conditions although was slower than the homoprocess. The copolymer of about the double molecular weight in comparison with the previously synthesized PBA was finally obtained according to GPC data shown in Figure 7.

The GPC traces of the first synthesized PBA revealed bimodal MWD, as mentioned above, and only the principal peak was shifted to the higher molecular weights after the copolymerization with St. The secondary peak with $M_n \approx 3 \times 10^6$ did not practically move, meaning that it was composed by dead polymer chains. The ^{1}H NMR spectrum revealed the presence of both BA and St units in the copolymer (Figure 7a). The composition calculated from the NMR data gave F_{St} = 0.33 and F_{BA} = 0.67.

Simultaneous Copolymerization of St and BA. When an equimolar mixture of BA and St in MEK (the feed composition f_{BA} = 0.5 and f_{St} = 0.5) was irradiated at room temperature at the initial molar ratio of $[BA]_0/[St]_0/[I]_0/[EBiB]_0$ = 150/150/1/1, both monomers were almost equally consumed in spite of a big difference in their homopolymerization rates. According to the GC data, the consumptions of BA and St were 11% and 13%, respectively, resulting in 24% total conversion after 10 h. Thus, the copolymerization was faster than the homopolymerization of St but much slower than that of BA. The ^{1}H NMR spectrum of the copolymer and the corresponding GPC chromatogram are depicted in Figure 8.

Interestingly, MWD was monomodal in this case; just one fairly symmetrical peak can be seen in the chromatogram as opposed to the BA homopolymerization. The ^{1}H NMR spectrum was very similar to the spectra reported for statistical BA/St copolymer produced by free radical process.[57,58] The $-OCH_2$ protons of BA units appeared as a broad triplet around 3.5−4.1 ppm, whereas a signal from these protons in the block copolymer appeared as a much narrower singlet at 4.1 ppm (see Figure 6) as for homo-PBA. This may be considered as an additional evidence for the formation of PBA-*b*-PSt in the photoprocess. The copolymer produced by simultaneous polymerization was slightly enriched by St units in accordance with the GC consumption data: composition of F_{St} = 0.59 and F_{BA} = 0.41 was determined from the ^{1}H NMR spectrum. A rough estimation based on simple terminal model using r_{St} = 0.698 and r_{BA} = 0.164, i.e. the reactivity ratios reported for the conventional radical copolymerization at 50 °C,[59] gave values of F_{St} = 0.59 and F_{BA} = 0.40, which are in good agreement with our experimental data. The simultaneous photopolymerization of St and BA was also carried out at 60 °C, and a conversion of about 40% was reached in this case after 6 h. The copolymer composition was significantly the same: F_{St} = 0.60 and F_{BA} = 0.40. ^{13}C NMR characterization is important for this copolymer because it may be used for qualitative determination of the monomer sequences distribution.[57,58] The carbonyl carbon $(C{=}O)_{BA}$ resonance signal around 175 ppm is particularly informative because it is not sensitive to stereochemical effects. The ^{13}C NMR spectrum for the BA-St copolymer obtained in the photopolymerization is shown in Figure 9. The expanded region around 175 ppm indicates a strong tendency to alternation since the sequence of St−BA−St predominates in the spectrum. Features such as a deceleration of the polymerization with an increase of St in the feed, the essential independence of the polymer composition with the temperature, similar to that observed in the ruthenium-catalyzed simultaneous photopolymerization of BA with St, have been reported for free radical copolymerization of this pair of

dx.doi.org/10.1021/ma3014383 | *Macromolecules* 2012, 45, 8135−8146

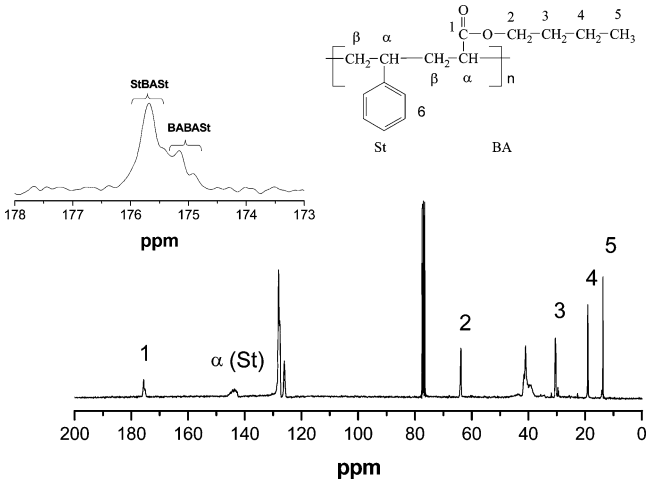

Figure 9. ^{13}C NMR spectrum in $CDCl_3$ of copolymer of St and BA obtained by simultaneous polymerization under visible light irradiation at room temperature.

monomers.[60−62] Their copolymerization by atom transfer radical process with copper-based catalysts was also deeply investigated.[63−65] Although controlled radical polymerization has its own peculiarities, such as the persistent radical effect and obtaining of low molecular weight polymer at low conversion which can affect the course of the copolymerization, the authors concluded that the reaction proceeded through carbon-centered radicals and that the main kinetic features and copolymer composition could be described satisfactorily by models developed for the free radical process. All these conclusions are valid for the reported ruthenium-catalyzed photopolymerization of the St−BA pair.

Effect of Visible Light on the Polymerization. As mentioned above, the polymerization did not proceed under postirradiation conditions, i.e., when system was initially irradiated by visible light and then kept at 40 °C without irradiation. No further increase in conversion or changes in the molecular weights were detected. The experiments with consecutive alternation of periods when the light was turned on and off were also carried out. It was found that the extension of the period of "darkness" had a crucial influence on the polymerization kinetics.

As shown in Figure 10, the polymerization ceased immediately upon switching off, and the reaction proceeded again when the light was turned on after 20 min with practically the same rate as observed under conditions of the continuous irradiation. However, at more extended periods of "darkness" the polymerization reinitiated at a much slower rate and almost did not reinitiate when the "dark" period lasted for 1 h, indicating possible side reactions.

Mechanistic Approach. In order to get a better insight into the mechanism of the photocatalysis, the behavior of complex **I** upon the irradiation in acetone was investigated by cyclic voltammetry and ^1H NMR. The cyclic voltammogram of **I** obtained at a glassy carbon working electrode in acetone in the potential range from −1 to +1 versus Ag/AgCl in the absence of irradiation is characterized by a single quasi-reversible $Ru^{II/III}$ redox feature with $E_{1/2}$= 740 mV (line a in Figure 11). Its CV changed when the solution was irradiated by visible light for only 30 min. The original well-defined redox wave disappeared, and a new one developed simultaneously at 580 mV (line b in Figure 11). The changes were similar to

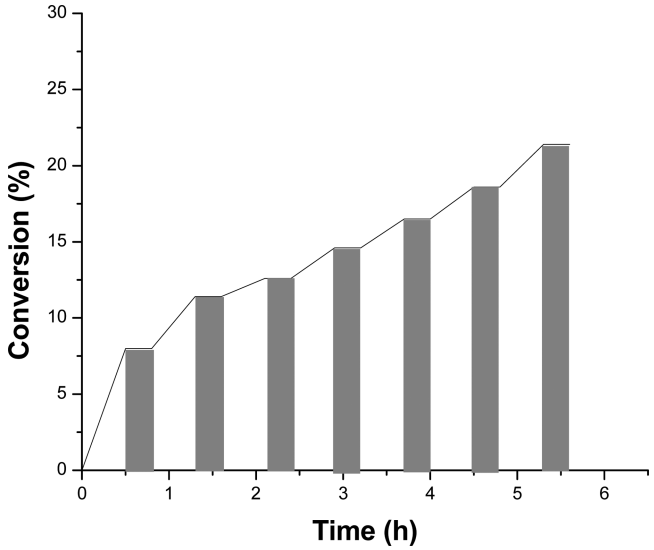

Figure 10. Effect of visible light irradiation during the polymerization of MMA with **I** and EB*i*B in acetone at room temperature; $[MMA]_0/[\mathbf{I}]_0/[EBiB]_0$ = 200/1/1, MMA/acetone 50% v/v. The shaded regions indicate the periods when the lamp was turned off.

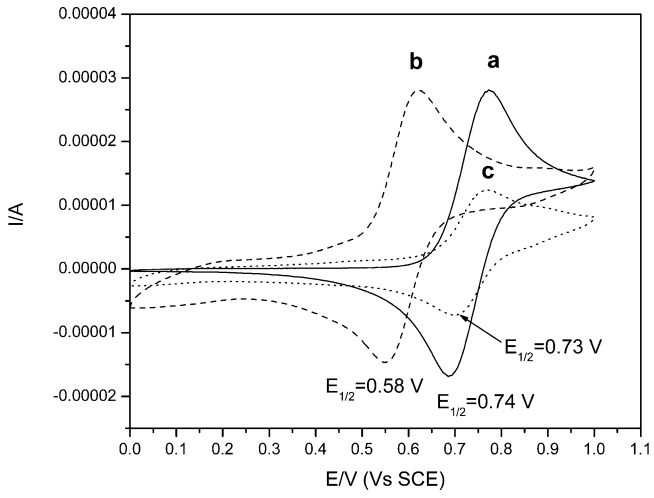

Figure 11. Cyclic voltammograms of **I** (3 mM) in acetone before (a, solid line), after 30 min of irradiation (b, dashed line), and after 4 h storage without irradiation at room temperature (c, dotted line); 0.1 M *n*-Bu_4NPF_6, glassy carbon electrode, scan rate 0.1 V s^{-1}; room temperature.

those monitored in MeOH upon visible light irradiation for this complex,[47] but the overall potential drop in acetone was not as drastic as that in MeOH (160 mV in acetone vs 800 mV in MeOH). By analogy to the phenomenon occurring in MeOH, we assumed a photochemical solvolysis of MeCN ligands. However, it is probable that only one MeCN ligand was substituted by acetone, as the observed drop in the reduction potential is comparable to that in MeOH when a single MeCN ligand was substituted.[47]

This hypothesis was confirmed by ^1H NMR measurements before and after irradiation of **I** in a carefully deoxygenated solution of $(CD_3)_2CO$. The spectrum of intact **I** (Figure 12) showed two resonances at 2.49 and 2.32 from MeCN ligands. After irradiation, both aromatic and aliphatic areas of the spectrum changed. In the aromatic region, signal from the original **I** at 9.92 ppm disappeared and two slightly broad new

dx.doi.org/10.1021/ma3014383 | *Macromolecules* 2012, 45, 8135−8146

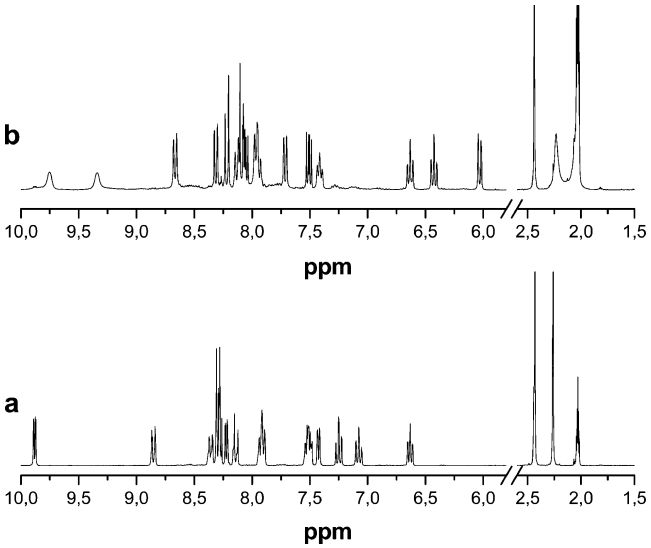

Figure 12. ^{1}H NMR spectra of **I** in $(CD_3)_2CO$ before (a) and after 2 h of irradiation by visible light (b).

ones at 9.80 and 9.38 ppm arose (possibly reflecting a dynamic process). Other aromatic signals were shifted, but the aromatic proton count remained the same; viz. there were total 16 protons (8 from phpy + 8 from phen) before and after irradiation. In the aliphatic region, only one signal from the coordinated MeCN at 2.50 ppm remained. Monitoring of the resonance from free MeCN at 2.05 ppm was difficult in $(CD_3)_2CO$ because of the signals from the residual acetone.[66] Thus, we believe that the irradiation caused a substitution of only one of two acetonitrile ligands by acetone.

It is worth noting that the time needed for complete conversion is shorter when the photosolvolysis was studied electrochemically than it was monitored by NMR. This may be due to a salt effect on the kinetics of photochemical ligand substitution since the electrochemical experiments were performed in the presence of 0.1 M Bu_4NPF_6.[67] The influence of salts on the reaction rate is currently under active investigation. The ^{1}H NMR spectrum of irradiated **I** stored for 4 h at room temperature was complicated and ill-defined, probably due to the formation of paramagnetic Ru^{III} species or/and oligomerization.[68,69]

Changes on storage were also followed by cyclic voltammetry. As shown in Figure 11, the photochemically generated complex **I″** is not stable in the absence of irradiation; it is gradually converted into a novel species characterized by a higher potential (voltammogram **c** in Figure 11). Irradiation of this novel compound did not cause any notable changes in its CV, meaning that it is not the original **I** in spite of their very close reduction potentials. Interestingly, the irreversible "**b**" to "**c**" conversion did not occur under continuous irradiation and "species **b**" (**I″**) was conserved for quite a prolonged period of time.

The results obtained by ^{1}H NMR and cyclic voltammetry are consistent and allow us to suggest the unified mechanism of photocatalysis (Scheme 2). It is important to keep in mind that there is no polymerization in the "dark" (see Figure 10). The mechanism in Scheme 2 consists of two major events, i.e., photochemical events, which result in generation of the active species **I′**, and metal-catalyzed radical polymerization (ATRP) events. Combination of both these processes provides the controlled polymerization.

The photochemical events start with the generation of solvento species **I″** through the intermediacy of 16e species **I′** because the photosolvolysis of Ru^{II} complexes occurs via a dissociative mechanism typical of substitutions in octahedral transition metal complexes.[70] The crystallographic results show that the Ru−NCMe bond trans to the 2-phenylpyridine nitrogen is about 10% longer than that trans to the phen nitrogen.[47] This suggests that MeCN trans to the 2-phenylpyridine will dissociate preferably in weakly coordinating solvents. The dissociation generates a reactive 16e intermediate **I′**, which readily coordinates acetone affording **I″** (Scheme 2). The **I** to **I″** conversion is practically irreversible within the time scale explored because recoordination of organic nitriles to Ru^{II} occurs very slow.[47,70] Though irradiation results in practically complete transformation of **I** into **I″**, the latter species cannot

Scheme 2. A General Mechanism of Polymerization Catalyzed by Photolabile Cyclometalated Ru^{II} Complexes in Acetone that Consists of Photochemical and ATRP Events (See Text for Explanation)

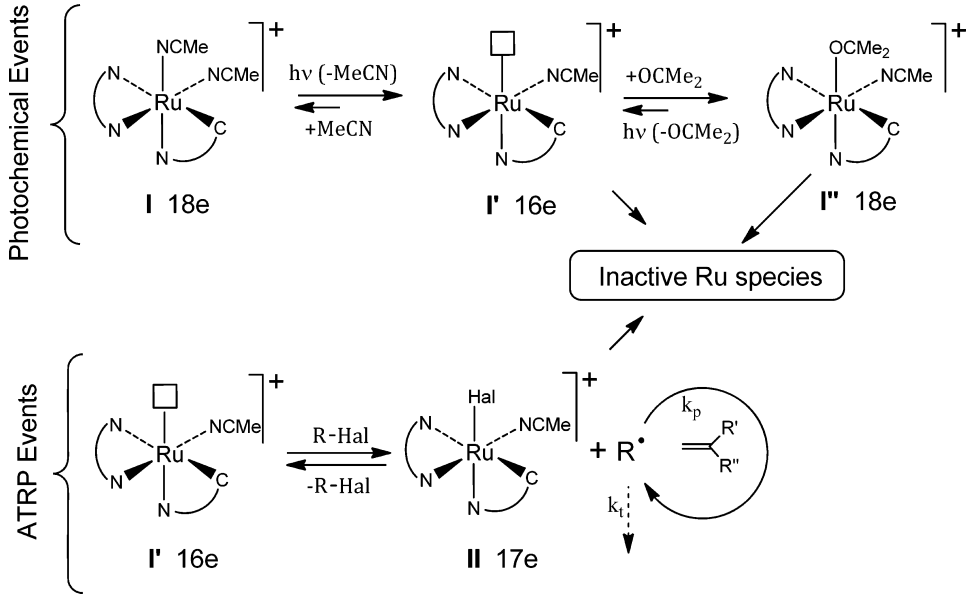

dx.doi.org/10.1021/ma3014383 | *Macromolecules* 2012, 45, 8135−8146

be regarded as a true intermediate because the polymerization still requires light. This is why we assume that the light is essential for generating a coordinatively unsaturated 16e intermediate such as **I′** from **I″**. As shown in Scheme 2, complex **I′** results from the photoinduced dissociation of acetone because it is the weakest ligand coordinated to ruthenium. However, a release of MeCN cannot be presently ruled out.

In any case the 16e intermediate produced opens a channel for the radical polymerization events via atom transfer approach because the vacant site at Ru^{II} is an entry for the halide from the initiator to produce 17e complex **II** as a result of 1e oxidative addition of R-Hal. The control in the polymerization in a great extent determined by low concentration of the intermediate **I′**.

The mechanism in Scheme 2 provides also a clue for the catalysts exhaustion during the polymerization. According to the ^{1}H NMR data, about 35% of the complex was lost after 6 h of polymerization. Acetone is a weakly coordinating ligand, and therefore **I″** may rearrange into catalytically inactive, stable dimeric complexes, as it has been reported for this and other Ru^{II} compounds[47,68,69] or suffer degradation processes. In principle, intermediates **I′** and **II** may also collapse during the polymerization, but these pathways should not be dominant ones because both **I′** and **II** are produced in minute amounts. The loss does not however affect the polymerization appreciably because the conversion is nevertheless high. That also may be interrelated in favor of the hypothesis on **I′** as a true catalytic species whose concentration maintained relatively constant through the dynamic equilibrium with solvento species **I″**.

Undesirable reactions of the complex are inevitable in this method, but their percentage may be decreased, and therefore, the efficiency of the catalyst may be significantly increased. For instance, we are currently evaluating the use of some additives and use of more coordinating solvents, instead of acetone.

CONCLUSIONS

Radical polymerizations of three typical hydrophobic monomers—MMA, St, and BA—were successfully performed using phototriggered precatalysts and alkyl halide as initiator at low temperatures in acetone and MEK. The polymerizations proceeded under continuous irradiation by visible light and immediately stopped when the light was turned off. The molecular weights grew with conversion, and PDIs were relatively narrow for MMA and St. GPC analysis showed monomodal MWD in the polymerizations of MMA and St, but the polymerization of BA resulted in bimodal MWD with the principal peak gradually shifting to the higher molecular weights with conversion. MMA and BA were polymerized at ambient temperature, and high conversions for both monomers were achieved. Polymerization of BA was particularly fast affording 90% conversion in 8 h. Polymerization of St was very slow at room temperature but proceeded at higher rate at 60 °C. Block copolymers of MMA and BA with St, PMMA-*b*-PSt, and PBA-*b*-PSt were synthesized, confirming the living character of the polymerizations.

A mechanism of the photocatalysis based on the behavior of the ruthenium complex in acetone under visible light irradiation has been suggested, and several elemental steps are likely to be involved. Photoinduced substitution of one MeCN ligand by a molecule of acetone through a very active 16-electron species is presumably the key step for the polymerizations at low temperature. Continuous irradiation is needed to maintain equilibrium between acetone coordinated and the coordinatively unsaturated species. Despite that such subtle mechanism resulted in lower than 100% initiation efficiency, we believe that the careful choice of the solvent and of a photosensitive ruthenium catalyst allowed us to design a new efficient, light-controlled, polymerization system.

AUTHOR INFORMATION

Corresponding Author

*E-mail: laz@servidor.unam.mx.

Notes

The authors declare no competing financial interest.

ACKNOWLEDGMENTS

This work was supported by CONACyT (projects 60610, 129801, and 153151 and scholarship to N. Vargas Alfredo) and PAPIIT (grants IN102810 and IN204812). The authors are grateful to Q. M.A. Peña Gonzales (Instituto de Química, UNAM) and I. Q. G. Cedillo Valverde (Instituto de Investigaciones en Materiales, UNAM) for the NMR measurements.

REFERENCES

(1) Kato, M.; Kamigaito, M.; Sawamoto, M.; Higashimura, T. *Macromolecules* **1995**, *28*, 1721−1723.
(2) Wang, J.-S.; Matyjaszewski, K. *J. Am. Chem. Soc.* **1995**, *117*, 5614−5615.
(3) Tsarevsky, N. V.; Braunecker, W. A.; Tang, W.; Brooks, S. J.; Matyjaszewski, K.; Weisman, G. R.; Wong, E. H. *J. Mol. Catal. A: Chem.* **2006**, *257*, 132−140.
(4) Pintauer, T.; Matyjaszewski, K. *Chem. Soc. Rev.* **2008**, *37*, 1087−1097.
(5) Tang, H.; Arulsamy, N.; Radosz, M.; Shen, Y.; Tsarevsky, N. V.; Braunecker, W. A.; Tang, W.; Matyjaszewski, K. *J. Am. Chem. Soc.* **2006**, *128*, 16277−16285.
(6) Ouchi, M.; Terashima, T.; Sawamoto, M. *Chem. Rev.* **2009**, *109*, 4963−5050.
(7) Yoda, H.; Nakatami, K.; Terashima, T.; Ouchi, M.; Sawamoto, M. *Macromolecules* **2010**, *43*, 5595−5601.
(8) Tsarevsky, N. V.; Matyjaszewski, K. *Chem. Rev.* **2007**, *107*, 2270−2299.
(9) Braunecker, W. A.; Matyjaszewski, K. *Prog. Polym. Sci.* **2007**, *32*, 93−146.
(10) Matyjaszewski, K.; Xia, J. *Chem. Rev.* **2001**, *101*, 2921−2990.
(11) Kamigaito, M.; Ando, T.; Sawamoto, M. *Chem. Rev.* **2001**, *101*, 3689−3745.
(12) Campagna, S.; Puntoriero, F.; Nastasi, F.; Bergamini, G.; Balzani, V. *Top. Curr. Chem.* **2007**, *280*, 117−214.
(13) Ivin, K. J.; Mol, J. C. In *Olefin Metathesis and Metathesis Polymerization*, 2nd ed.; Academic Press: San Diego, 1997; p 36.
(14) Trnka, T. M.; Grubbs, R. H. *Acc. Chem. Res.* **2001**, *34*, 18−29.
(15) Delaude, L.; Demonceau, A.; Noels, A. F. *Chem. Commun.* **2001**, *11*, 986−987.
(16) Grishin, I. D.; Grishin, D. F. *Russ. Chem. Rev.* **2008**, *77*, 633−648.
(17) Wang, D.; Wurst, K.; Knolle, W.; Decker, U.; Prager, L.; Naumov, S.; Buchmeiser, M. R. *Angew. Chem., Int. Ed.* **2008**, *47*, 3267−3270.
(18) Ben-Asuly, A.; Aharoni, A.; Diesendruck, C. E.; Vidavsky, Y.; Goldberg, I.; Straub, B. F.; Lemcoff, N. G. *Organometallics* **2009**, *28*, 4652−4655.
(19) Delaude, L.; Szypa, M.; Demonceau, A.; Noels, A. F. *Adv. Synth. Catal.* **2002**, *344*, 749−756.
(20) Karlen, T.; Ludi, A.; Mühlebach, A.; Bernhard, P.; Pharisa, C. *J. Polym. Sci., Part A: Polym. Chem.* **1995**, *33*, 1665−1674.

(21) Van der Schaaf, P. A.; Hafner, A.; Mühlebach, A. *Angew. Chem., Int. Ed. Engl.* **1996**, *35*, 1845−1847.
(22) Subbotina, I. R.; Shelimov, B. N.; Kazansky, V. B. *Kinet. Catal.* **1997**, *38*, 678−684.
(23) Tarasov, A. L.; Shelimov, B. N.; Kazansky, V. B.; Mol, J. C. *J. Mol. Catal. A: Chem.* **1997**, *115*, 219−228.
(24) Gromada, J.; Spanswick, J.; Matyjaszewski, K. *Macromol. Chem. Phys.* **2004**, *205*, 551−566.
(25) Monge, S.; Darcos, V.; Haddleton, D. M. *J. Polym. Sci., Part A: Polym. Chem.* **2004**, *42*, 6299−6308.
(26) Quebatte, L.; Haas, M.; Solari, E.; Scopelliti, R.; Nguyen, Q. T.; Severin, K. *Angew. Chem., Int. Ed.* **2005**, *44*, 1084−1088.
(27) Simal, F.; Demonceau, A.; Noels, A. F. *Angew. Chem., Int. Ed.* **1999**, *38*, 538−540.
(28) De Clercq, B.; Verpoort, F. *Macromolecules* **2002**, *35*, 8943−8947.
(29) Zhang, H.; Schubert, U. S. *J. Polym. Sci., Part A: Polym. Chem.* **2004**, *42*, 4882−4894.
(30) Wang, G.; Zhu, X.; Zhu, J.; Cheng, Z. *J. Polym. Sci., Part A: Polym. Chem.* **2006**, *44*, 483−489.
(31) Qin, S.-h.; Qin, D.-q.; Qiu, K.-y. *Chin. J. Polym. Sci.* **2001**, *19*, 441−445.
(32) Kwak, Y.; Matyjaszewski, K. *Macromolecules* **2010**, *43*, 5180−5183.
(33) Koumura, K.; Satoh, K.; Kamigaito, M. *Polym. Prepr.* **2005**, *49*, 230−231.
(34) Koumura, K.; Satoh, K.; Kamigaito, M. *Macromolecules* **2008**, *41*, 7359−7367.
(35) Tasdelen, M. A.; Uygun, M.; Yagci, Y. *Macromol. Rapid Commun.* **2011**, *32*, 58−62.
(36) Diaz Camacho, F.; Le Lagadec, R.; Ryabov, A.; Alexandrova, L. *J. Polym. Sci., Part A: Polym. Chem.* **2008**, *46*, 4193−4204.
(37) Aguilar-Lugo, C.; Le Lagadec, R.; Ryabov, A. D.; Cedillo Valverde, G.; Lopez Morales, S. *J. Polym. Sci., Part A: Polym. Chem.* **2009**, *47*, 3814−3629.
(38) Gonzalez Diaz, M. O.; Lopez Morales, S.; Le Lagadec, R.; Alexandrova, L. *J. Polym. Sci., Part A: Polym. Chem.* **2011**, *49*, 4562−4577.
(39) Ouchi, M.; Terashima, T.; Sawamoto, M. *Acc. Chem. Res.* **2008**, *41*, 1120−1132.
(40) Ando, T.; Kamigaito, M.; Sawamoto, M. *Macromolecules* **2000**, *33*, 5825−5829.
(41) Braunecker, W. A.; Brown, W. C.; Morelli, B. C.; Tang, W.; Poli, R.; Matyjaszewski, K. *Macromolecules* **2007**, *40*, 8576−8585.
(42) Motoyama, Y.; Hanada, S.; Shimamoto, K.; Nagashima, H. *Tetrahedron* **2006**, *62*, 2779−2788.
(43) Motoyama, Y.; Hanada, S.; Niibayashi, S.; Shimamoto, K.; Takaoka, N.; Nagashima, H. *Tetrahedron* **2005**, *61*, 10216−10226.
(44) O'Reilly, R. K.; Gibson, V. C.; White, A. J. P.; Williams, D. J. *Polyhedron* **2004**, *23*, 2921−2928.
(45) Ouchi, M.; Ito, M.; Kamemoto, S.; Sawamoto, M. *Chem.—Asian J.* **2008**, *3*, 1358−1364.
(46) Opstal, T.; Verpoort, F. *Angew. Chem., Int. Ed.* **2003**, *42*, 2876−2879.
(47) Ryabov, A. D.; Le Lagadec, R.; Estevez, H.; Toscano, R. A.; Hernandez, S.; Alexandrova, L.; Kurova, V. S.; Fischer, A.; Sirlin, C.; Pfeffer, M. *Inorg. Chem.* **2005**, *44*, 1626−1634.
(48) Delaude, L.; Delfosse, S.; Richel, A.; Demonceau, A.; Noels, A. F. *Chem. Commun.* **2003**, *39*, 1526−1527.
(49) Tutusaus, O.; Delfosse, S.; Simal, F.; Demonceau, A.; Noels, A. F.; Nuñez, R.; Viñas, C.; Teixidor, F. *Inorg. Chem. Commun.* **2002**, *5*, 941−945.
(50) Richel, A.; Tutusaus, O.; Viñas, C.; Teixidor, F.; Demonceau, A.; Noels, A. F. *Polym. Prepr.* **2005**, *46*, 227−228.
(51) Shold, D. M.; Rebbert, R. E. *J. Photochem.* **1978**, *9*, 499−517.
(52) Alapi, T.; Van Craeynest, K.; Van Langenhoeve, H.; Dewulf, J.; Dombi, A. *Chemosphere* **2007**, *66*, 139−144.
(53) Dursun, C.; Degirmenci, M.; Yagci, Y.; Jockusch, S.; Turro, N. J. *Polymer* **2003**, *44*, 7389−7396.
(54) Pascual, S.; Coutin, B.; Tardi, M.; Polton, A.; Vairon, J.-P. *Macromolecules* **1999**, *32*, 1432−1437.
(55) Yamauchi, K.; Lizotte, J. R.; Long, T. E. *Macromolecules* **2003**, *36*, 1083−1088.
(56) (a) Uegaki, H.; Kotani, Y.; Kamigaito, M.; Sawamoto, M. *Macromolecules* **1997**, *30*, 2249−2253. (b) Ando, T.; Kamigaito, M.; Sawamoto, M. *Tetrahedron* **1997**, *53*, 15445−15457. (c) Nagaki, A.; Kawamura, K.; Suga, S.; Ando, T.; Sawamoto, M.; Yoshida, J.-i. *J. Am. Chem. Soc.* **2004**, *126*, 14702−114703. (d) Bon, S. A. F.; Steward, A. G.; Haddleton, D. M. *J. Polym. Sci., Part A: Polym. Chem.* **2000**, *38*, 2678−2686. (e) Delfosse, S.; Borguet, Y.; Delaude, L.; Demonceau, A. *Macromol. Rapid Commun.* **2007**, *28*, 492−503. (f) Qin, D.-Q.; Qin, S.-H.; Qiu, K.-Y. *J. Polym. Sci., Part A: Polym. Chem.* **2001**, *39*, 3464−3473.
(57) Llauro-Darricades, M. F.; Pichot, C.; Gillot, J.; Rios, L. G.; Cruz, M. A. E.; Guzman, C. *Polymer* **1986**, *27*, 889−898.
(58) Brar, A. S.; Sunitra; Satyanarayana, C. V. V *Polym. J.* **1992**, *24*, 879−887.
(59) Kaszás, G.; Földes-Berezsnich, T.; Tüdos, F. *Eur. Polym. J.* **1984**, *20*, 395−398.
(60) Dubé, M. A.; Penlidis, A.; ÓDriscoll, K. F. *Chem. Eng. Sci.* **1990**, *45*, 2785−2792.
(61) Fernández-García, M.; Fernández-Sanz, M.; López Madruga, E.; Fernández-Monreal, C. *Macromol. Chem. Phys.* **1999**, *200*, 199−205.
(62) Kostanski, L. K.; Hamielec, A. E. *Polymer* **1992**, *33*, 3706−3710.
(63) Arehart, S. V.; Matyjaszewski, K. *Macromolecules* **1999**, *32*, 2221−2231.
(64) Chambard, G.; Klumperman, B. *ACS Symp. Ser.* **2000**, *768*, 197−210.
(65) Chambard, G.; Klumperman, B. *Polym. Prepr.* **2002**, *43*, 9−10.
(66) Gottlieb, H. E.; Kotlyar, V.; Nudelman, A. *J. Org. Chem.* **1997**, *62*, 7512−7515.
(67) Loupy, A.; Tchoubar, B. *Salt Effects in Organic and Organometallic Chemistry*, 1st ed.; Wiley-VCH: Weinheim, 1992; p 77.
(68) Jurss, J. W.; Concepcion, J. J.; Butler, J. M.; Omberg, K. M.; Baraldo, L. M.; Thompson, D. G.; Lebeau, E. L.; Hornstein, B.; Schoonover, J. R.; Jude, H.; Thompson, J. D.; Dattelbaum, D. M.; Rocha, R. C.; Templeton, J. L.; Meyer, T. J. *Inorg. Chem.* **2012**, *51*, 1345−1358.
(69) Warren, J. T.; Chen, W.; Johnston, D. H.; Turro, C. *Inorg. Chem.* **1999**, *38*, 6187−6192.
(70) Durham, B.; Walsh, J. L.; Charles, L. C.; Meyer, T. J. *Inorg. Chem.* **1980**, *19*, 860−865.